Int. J. Solids Structures Vol. 21, No. 4, pp. 399–410, 1985
Printed in the U.S.A.

0020–7683/85 $3.00 + .00

A NORMALLY LOADED HALF-PLANE WITH AN EDGE CRACK

D. A. HILLS† and MARIA COMNINOU
Department of Mechanical Engineering and Applied Mechanics, University of Michigan, Ann Arbor, MI 48109, U.S.A.

(*Received* 28 *November* 1983; *in revised form* 24 *May* 1984)

Abstract—An elastic half-plane is subjected to a uniform pressure over part of its surface. A normal edge crack is assumed to lie at the edge of the loaded region. The effect of Coulomb friction between the crack faces is considered, and the various possibilities involving stick and slip regions along the crack are examined. Stress intensity factors are obtained.

INTRODUCTION

The study of brittle or fatigue fracture that involves contact along the crack faces is difficult for several reasons. On the one hand, material data pertaining to the growth of cracks in a compressive environment are scant, and, on the other, frictional stresses may be transmitted across the contacting crack faces. The analysis of cracks under these conditions is complicated. Nevertheless, solutions to some idealized problems involving a layer-substrate geometry[1–4] or a subsurface crack parallel to the free surface[5] have been presented. In the present study, we examine the case of a crack perpendicular to the surface of the half-plane. This geometry is motivated by the following application. When a component suffers impact loading, little wear occurs other than by some surface degradation in the form of surface cracks[6]. These may form anywhere within the contact zone. However, it is found that if the load is imposed by a punch of high rigidity, or if there is a small additional shear present[7], the crack tends to grow in a plane delimiting the extent of loading. In the present calculation, only cracks at this location will be considered, since this reduces the number of independent variables, and the severest state of orthogonal shear is found here.

Figure 1 shows the four possible cases that might obtain. If there is a stick zone, it is found that this will always be attached to the upper end a of the crack. Note that cases IIa and IIb are similar, since if the crack is locked at the upper end, it is immaterial whether the incision extends to the free surface or stops short. It also transpires that the normal traction $N(x)$ transmitted across the crack is always negative, i.e. that the crack is always closed, and hence the slip zones may be modeled in terms of continuous distributions of glide dislocations alone.

BILATERAL SOLUTION

If the coefficient of interfacial friction f between the crack faces is extremely large, then shear tractions of any value may be transmitted. Under these conditions the crack has no influence, and the bilateral solution is given by a direct integration of Flamant's solution for a point force. Along the line $y = 0$;

$$\frac{\tau_{xy}}{p_0} = \frac{1}{\pi}\frac{L^2}{x^2 + L^2} \tag{1}$$

$$\frac{\sigma_{yy}}{p_0} = \frac{1}{\pi}\left[\frac{xL}{x^2 + L^2} - \tan^{-1}\left(\frac{L}{x}\right)\right]. \tag{2}$$

† Permanent address: Department of Engineering Science, Oxford University, Parks Road, Oxford, England.

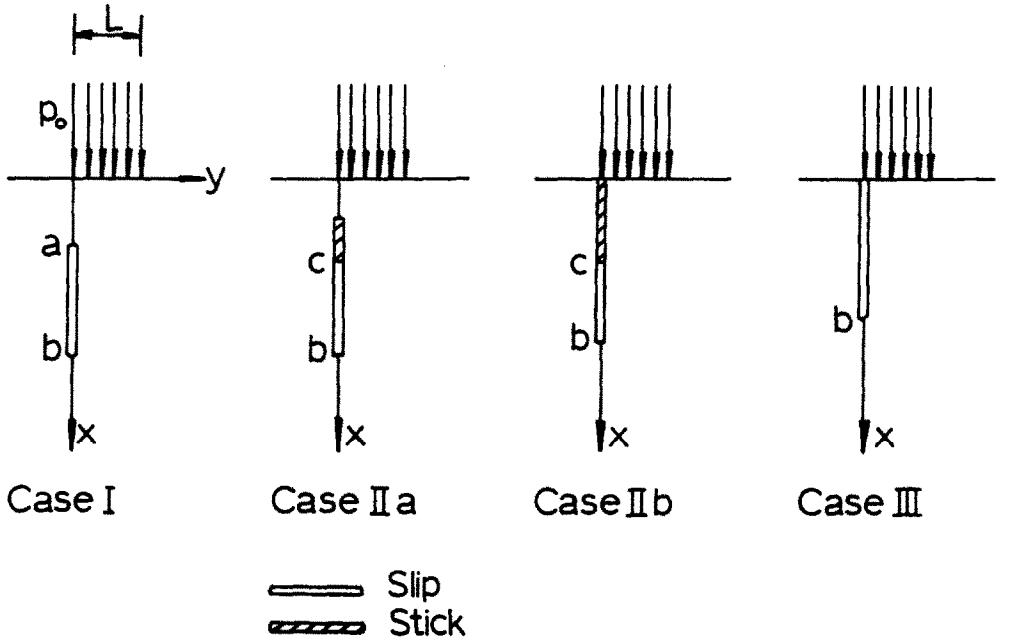

Fig. 1. Possible regimes of crack response and loading geometry.

For sufficiently large x, $|\tau_{xy}| > |f\sigma_{yy}|$, and hence if the lower crack tip is located deeply enough, there will always be some slip between the crack faces. For a crack of finite length, the stick condition is always violated at the lower end first. The slip zone starts there and extends upward as the coefficient of friction is reduced; it is independent of the applied pressure.

As pointed out by one of the reviewers, the limit of the bilateral solution at $x = y = 0$ depends upon the limiting sequence chosen and hence not much significance can be attached to it. A more realistic situation is that in which the crack is displaced a distance ϵ to the right or left of the origin, where ϵ is small in comparison with the other linear dimensions of the problem, L and b. For this case, eqns (1) and (2) must be modified by subtracting terms like those already shown but with L replaced by ϵ. The solution so obtained converges on that given in the paper as $\epsilon \to 0$. We note, however, that the requirement $\epsilon \ll b$ becomes more stringent when b is small. For example, for $|\epsilon| = 0.001$, significant variations from the results shown are obtained when b is < 0.1. Cracks that start inside the loaded region tend to stick at the surface, whereas those outside slip to the surface. In both cases, the stress intensity factors fall as the magnitude of ϵ increases. This is probably the reason that cracks are observed at the edge of the loaded region.

UNILATERAL SOLUTION

Case I

As in previous formulations[1–3, 5], the slip zones are modeled by the distribution of glide dislocations. In the present problem, the glide plane is perpendicular to the free surface, which is a special case of the dislocation near an interface, treated by Dundurs and Sendeckyj[8]. These results may be used, together with the appendix to a paper by Dundurs and Mura[9], to find the stresses generated on the glide plane. For a dislocation located at a point ξ of Burgers vector b_x, these stresses are

$$\sigma_{xy} = \frac{2\mu b_x}{\pi(\kappa + 1)}\left[\frac{1}{x - \xi} - \frac{1}{x + \xi} - \frac{2\xi}{(x + \xi)^2} + \frac{4\xi^2}{(x + \xi)^3}\right] \tag{3}$$

$$\sigma_{yy} = 0, \tag{4}$$

where μ is the shear modulus and $\kappa = 3-4\nu$ for plane strain. It will be recognized immediately that as a consequence of eqn (4), the normal traction $N(x)$ across the crack is not influenced by the dislocation distribution, but remains at the value given by the bilateral solution [eqn (2)]. The net shear traction $S(x)$ is given by

$$S(x) = \tau_{xy} + \frac{2\mu}{\pi(\kappa + 1)} \int_{\substack{\text{slip} \\ \text{zone}}} B_x(\xi) K(x, \xi)\, d\xi, \tag{5}$$

where

$$K(x, \xi) = \frac{1}{x - \xi} - \frac{1}{x + \xi} - \frac{2\xi}{(x + \xi)^2} + \frac{4\xi^2}{(x + \xi)^3}. \tag{6}$$

Consider now case I (Fig. 1a) in detail. Since $\tau_{xy} > 0$ (for all x), we anticipate that forward slip will occur, and hence put

$$S(x) = -f\, N(x), \qquad a < x < b \tag{7}$$

where f is the coefficient of friction:
so that a combination of eqns (7), (1), (2) and (5) gives the integral equation

$$\frac{2\mu}{\pi(\kappa + 1)} \int_a^b B_x(\xi) K(x, \xi)\, d\xi = \frac{-p_0}{\pi} \left[-f \tan^{-1}\left(\frac{L}{x}\right) + \frac{L(L + fx)}{x^2 + L^2} \right]. \tag{8}$$

This is solved using the method set out by Erdogan *et al.*[10]. First, the interval of integration is normalized by making the substitutions

$$\frac{x}{L} = \delta s + \sigma, \qquad \frac{\xi}{L} = \delta r + \sigma,$$

where

$$\delta = \frac{b - a}{2L}, \qquad \sigma = \frac{b + a}{2L}. \tag{9}$$

It is then recognized[11] that since the stresses are singular at each end of the crack, so is the dislocation density, and this fundamental solution is incorporated by letting

$$B_x(r) = \phi(r)\,(1 - r^2)^{-1/2} \frac{p_0(\kappa + 1)}{2\mu} \tag{10}$$

so that eqn (8) becomes

$$\int_{-1}^{+1} K(s, r)\,(1 - r^2)^{-1/2}\, \phi(r)\, dr = \frac{-p_0}{\delta\pi} \left[-f \tan^{-1}\left(\frac{L}{x}\right) + \frac{1 + fx/L}{1 + (x/L)^2} \right]. \tag{11}$$

A further condition must be imposed to ensure the uniqueness of displacements:

$$\int_{-1}^{+1} B_x(r)\, dr = 0. \tag{12}$$

The integral in eqn (11) has a Cauchy kernel, and therefore integration points r_i and

collocation points s_k are chosen at[10]:

$$r_i = \cos\frac{(2i-1)\pi}{n}, \qquad i = 1, \ldots, n$$

$$s_k = \cos\frac{\pi k}{n}, \qquad k = 1, \ldots, n-1.$$

The discretized form of eqn (11) is now given by

$$\sum_{i=1}^{n} \frac{1}{n}\phi(r_i)K(s_k, r_i) = \frac{-1}{\delta\pi}\left[-f\tan^{-1}\left(\frac{L}{x_k}\right) + \frac{1 + fx_k/L}{1 + (x_k/L)^2}\right], \tag{13}$$

while condition (12) becomes

$$\sum_{i=1}^{n} \phi(r_i)\frac{\pi}{n} = 0. \tag{14}$$

Equations (13) and (14) were solved and the relative displacement $h(x)$ between the crack faces found by evaluating numerically

$$h(x_k) = -\int_a^{x_k} B_x(\xi)\,d\xi. \tag{15}$$

It was verified that $h(x_k) > 0$ for all x_k, and therefore the requirement that the slip direction and the shear stress $S(x)$ have the same sign is maintained.

The stress intensity factors at each crack tip were found, using Krenk's interpolation formulas[12]. We note that

$$\begin{aligned} K_{II}(b) &= p_0\sqrt{\tfrac{1}{2}(b-a)}\,\phi(1) \\ K_{II}(a) &= -p_0\sqrt{\tfrac{1}{2}(b-a)}\,\phi(-1) \end{aligned} \tag{16}$$

where

$$\begin{aligned} \phi(1) &= \frac{1}{n}\sum_{i=1}^{n} F_i\,\phi(r_i), \\ \phi(-1) &= \frac{1}{n}\sum_{i=1}^{n} F_i\,\phi(r_{n+1-i}) \end{aligned} \tag{17}$$

and

$$F_i = \frac{\sin\left([(2n-1)/4n]\,(2i-1)\pi\right)}{\sin\left([(2i-1)/4n]\pi\right)}.$$

The results obtained showing the effects of crack length and depth are given in Figs. 2 and 3. Figure 4 shows the critical coefficient of friction to cause incipient stick at end a of the crack, as a function of crack length.

Case II

If the coefficient of friction is higher than indicated by Fig. 4, a finite stick zone will be present, assumed to extend from $x = 0$ or $x = a$ (whichever is greater) to $x = c$. The formulation for this case is essentially the same, and will not be repeated in detail. However, it should be noted that the dislocation density is finite at c, so that

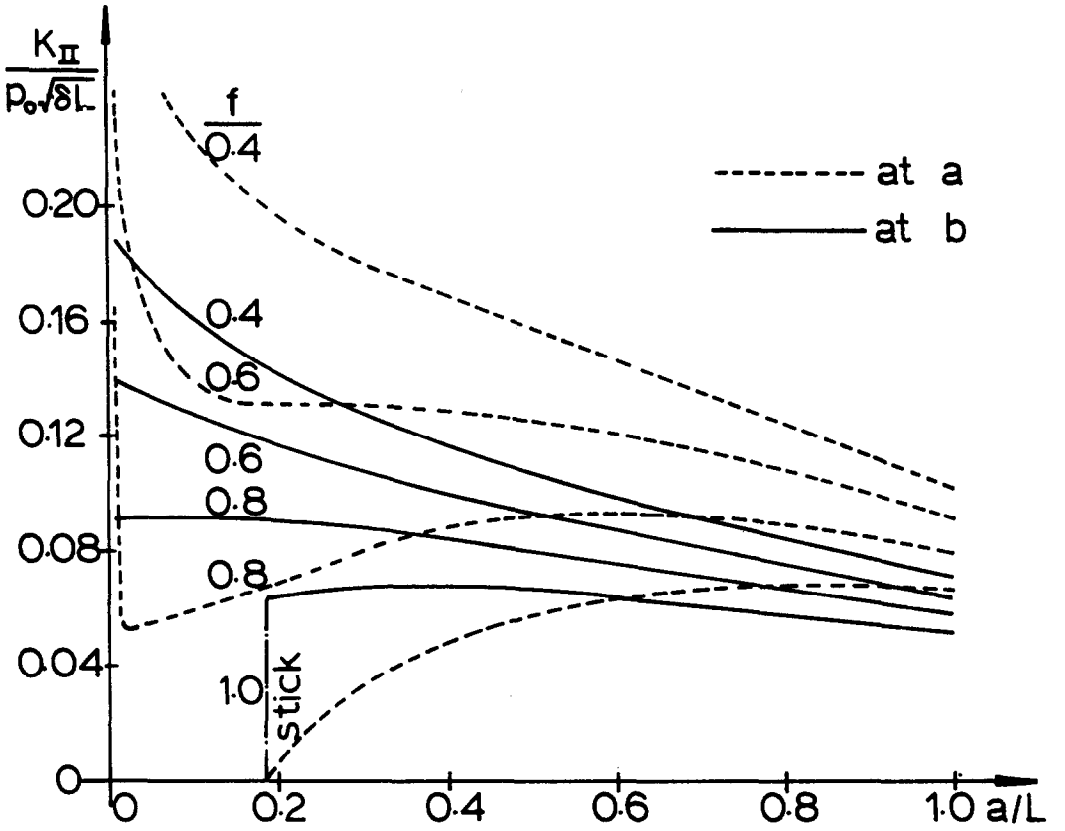

Fig. 2. Influence of crack depth on stress intensity factor [$(b - a)/L = 1$].

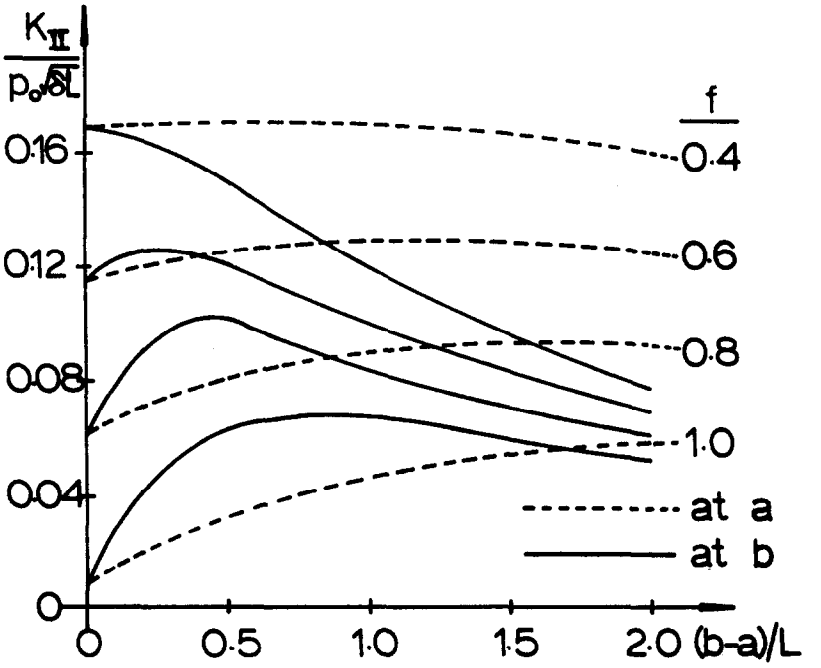

Fig. 3. Influence of crack length on stress intensity factor ($a/L = 0.4$).

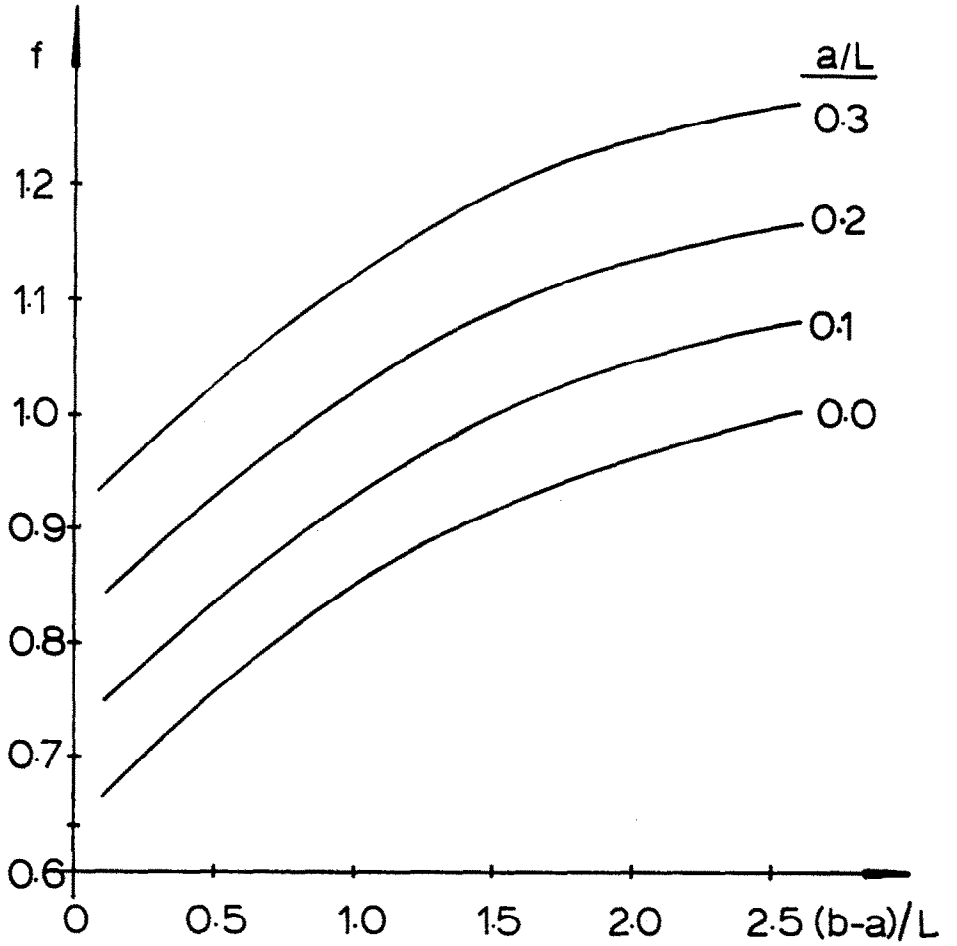

Fig. 4. Critical value of f, coefficient of interfacial friction, to cause stick for cracks at two depths.

the fundamental solution given in (10) becomes

$$B_x(r) = \phi(r)\,(1 - r)^{-\frac{1}{2}}\,(1 + r)^{\frac{1}{2}}\,p_0\,\frac{(\kappa + 1)}{2\mu}. \tag{18}$$

The normalizations of eqn (9) are now carried out with respect to the interval b–c. Further, the role played by eqn (12) is now to determine c (which is not known *a priori*).

The integration and collocation points are now given by[10]:

$$\begin{aligned} r_i &= \cos\frac{2i - 1}{2n + 1}\pi, \qquad i = 1, \ldots, n \\ s_k &= \cos\frac{2k\pi}{2n + 1}, \qquad k = 1, \ldots, n, \end{aligned} \tag{19}$$

while the discretized integral equation and auxiliary condition are

$$\begin{aligned} &\sum_{i=1}^{n}\frac{2(1 + r_i)}{2n + 1}\,\phi(r_i)\,K(s_i, r_i) = \frac{1}{\delta\pi}\left[f\tan^{-1}\left(\frac{L}{x_k}\right) - \frac{1 + fx_k/L}{(x_k/L)^2 + 1}\right] \\ &\sum_{i=1}^{n}\frac{2(1 + r_i)}{n}\,\pi\,\phi(r_i) = 0. \end{aligned} \tag{20}$$

The stress intensity factor for end b becomes

$$K_{II}(b) = p_0 \sqrt{\tfrac{1}{2}(b - c)}\, \phi(1). \tag{21}$$

Results for this case are given in Fig. 5.

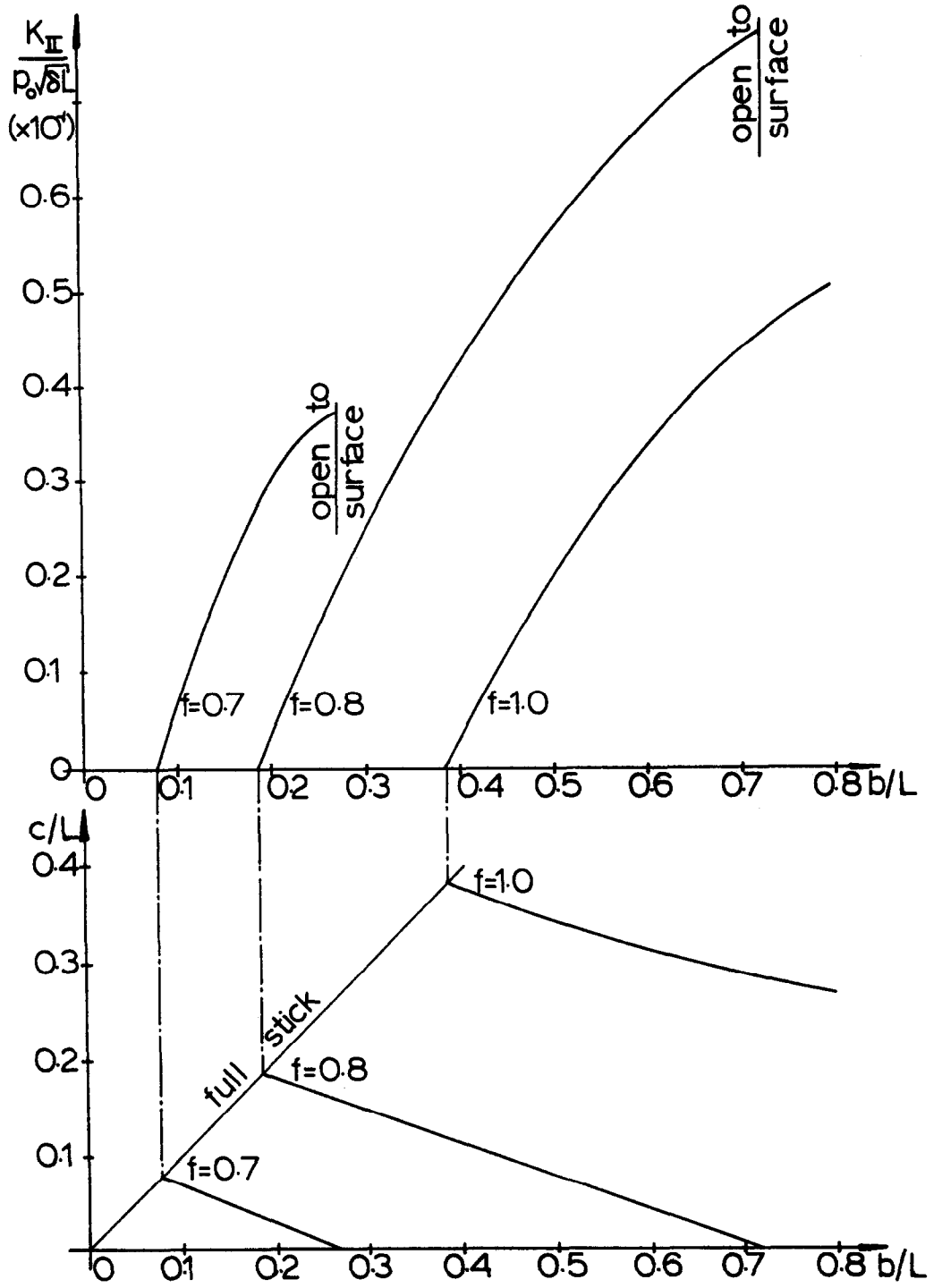

Fig. 5. Variation of stress intensity factor and position of stick/slip transition with friction and location of lower crack tip, for case II problems.

Case III

If the crack breaks the surface, and either the interfacial coefficient of friction is low or the crack is long, case III obtains. Here, we may initially write the dislocation density in the form

$$B_x(r) = \frac{\kappa + 1}{2\mu} p_0 \phi(r) (1 - r)^{-\frac{1}{2}} \tag{22}$$

but extend the range of definition of $B_x(r)$ to an even function along the negative axis[13], so that now eqn (10) may replace (22). $2n + 1$ integration points are chosen, and the contribution from the "central" $(n + 1)$th point is zero, so that

$$\sum_{i=1}^{n} \frac{1}{2n + 1} \psi(r_i) K(s_k, r_i) = \frac{1}{\pi b} \left[f \tan^{-1} \left(\frac{L}{x_k} \right) - \frac{1 + f x_k/L}{1 + (x_k/L)^2} \right], \tag{23}$$

where $\psi(r_i) = \phi(r_i)(1 + r_i)^{\frac{1}{2}}$.

The stress intensity factor at b may be found by Krenk's method, again putting the number of points equal to $2n + 1$. We find

$$K_{II}(b) = p_0 \psi(1) \sqrt{b}, \tag{24}$$

where

$$\psi(1) = \frac{1}{2n + 1} \left(\sum_{i=1}^{n} \left\{ \frac{\sin([(4n + 1)/(8n + 4)] (2i - 1)\pi)}{\sin([(2i - 1)/(8n + 4)]\pi)} \psi(r_i) + \frac{\sin([(4n + 1)/(8n + 4)] (2i + 2n + 1)\pi)}{\sin([(2i + 2n + 1)/(8n + 4)]\pi)} \psi(r_{n+1-i}) \right\} + \cos(n\pi) \psi(0) \right),$$

where $\psi(0)$ is conveniently found by linear extrapolation. Some results are given in Fig. 6.

DISCUSSION OF RESULTS

In the situation that motivated this analysis, there are so many independent variables that it is difficult to obtain a broad spectrum of representative results. However, by choosing the crack location as stated, which is where it is revealed by experiment, the number of variables is reduced to at most three: the interfacial coefficient of friction and the coordinates of the ends of the crack. If the crack breaks the free surface or is sufficiently near for locking of the upper end to occur, this number is reduced to two. Good continuity is found between results for the different regimes.

Figures 2 and 3 illustrate the effect of the depth of the crack and its length on the stress intensity factors for a buried crack that is slipping along its entire length. As the depth of the upper tip of the crack becomes vanishingly small (Fig. 2), the stress intensity factor there becomes infinite, which is physically reasonable since there is only an infinitesimal ligament of material to sustain the singular shear stress gradient. It will be noted that for the highest coefficient of interfacial friction chosen (viz. $f = 1.0$), as the crack is placed near the surface, there comes a point where the upper end of the crack begins to stick, i.e. when the stress intensity factor there falls to zero. This is illustrated in Fig. 4, which shows the critical combinations of f and crack length to cause stick, for two particular values of crack depth. It is interesting to note that the tendency to stick decreases with both crack length and depth. If the crack under consideration lies above the relevant line of Fig. 4, we need to consider results for the crack stuck at its upper end, which are shown in Fig. 5.

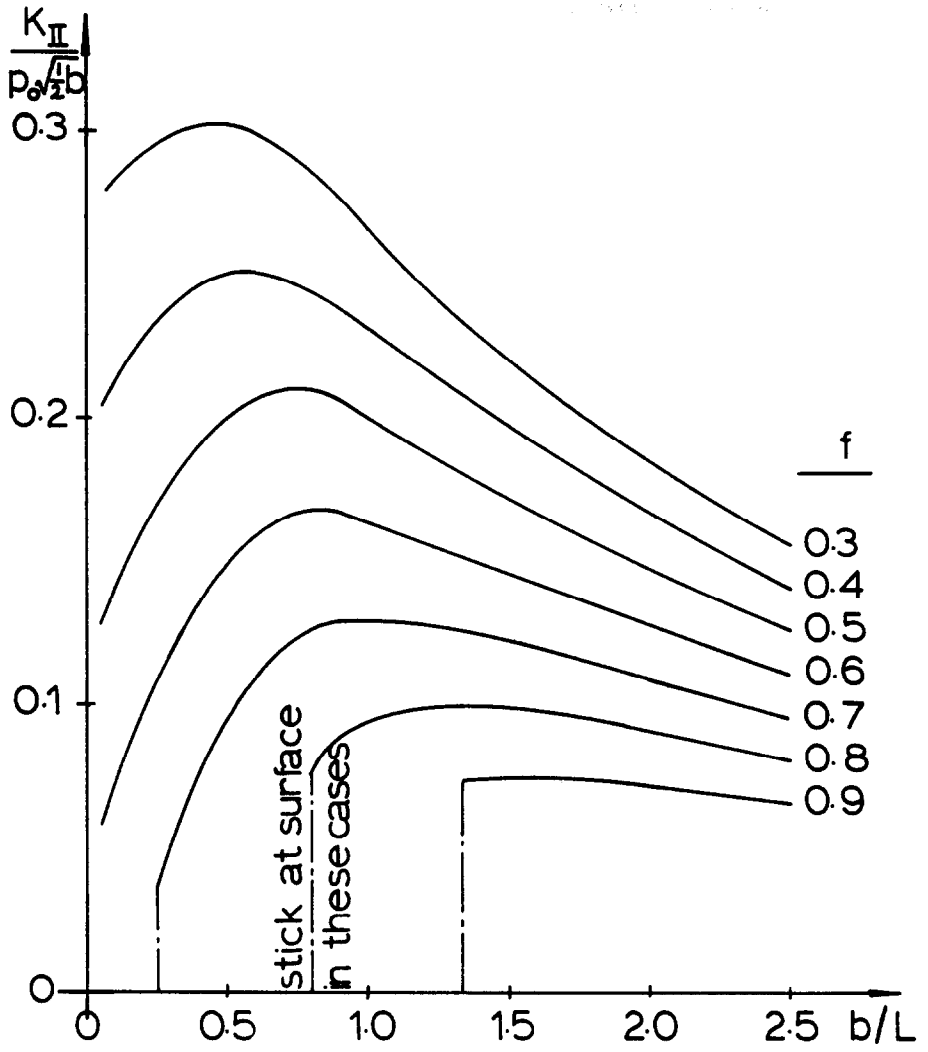

Fig. 6. Stress intensity factor for surface-breaking cracks that slip throughout their length (case III).

The only two independent variables are now f and b, the coordinate of the lower crack tip, and it is feasible to plot comprehensive results. For given values of f and b, the lower graph indicates the location of the stick/slip transition, whereas the upper graph shows the resultant stress intensity factor. It can be seen that in practice there are comparatively few cases where this regime obtains, since if $c \to b$, the crack remains locked along its entire length, whereas if $c \to 0$, the crack slips to the surface. The critical values of b and f for this latter case are seen to correspond to those predicted by Fig. 4 (onset of stick as $a \to 0$).

If the stick zone vanishes, then case III results (Fig. 6) are relevant. Figure 6 shows the stress intensity factors as a function of crack depth for various coefficient of friction values. It is found that there is a critically short crack where there is incipient stick at the surface, matching the values indicated by Figs. 4 (case I) and 5 (case II). These independent checks improve our confidence in the reliability of the results.

UNLOADING PHASE

A preliminary study was made of the unloading behavior of the cracks. It should be noted that since the value of the normal traction $N(x)$ is unmodified by the presence of glide dislocations, the final value of $N(x)$ as the load is removed completely is zero.

Thus, it will be impossible to support any residual shear, and the final stress state after unloading must be zero everywhere. In view of this conclusion, a comprehensive analysis was not thought worthwhile, and only one type of loading (case II) was considered.

Suppose that the maximum pressure sustained is p^*, and that a certain fraction λ of this is removed. Denoting

$$g_1(x) = \frac{1}{\pi}\frac{L^2}{L^2 + x^2}, \qquad g_2(x) = \frac{1}{\pi}\left[\frac{xL}{L^2 + x^2} - \tan^{-1}\left(\frac{L}{x}\right)\right], \tag{25}$$

the condition at maximum load will be

$$\begin{aligned} N^*(x) &= p^* g_2(x), \qquad a < x < b \\ S^*(x) &= -p^* f g_2(x). \end{aligned} \tag{26}$$

After relaxation by an amount λ, we have

$$\begin{aligned} S(x) &= -p^*[\lambda g_1(x) + f g_2(x)] \\ N(x) &= p^* g_2(x)(1 - \lambda). \end{aligned} \tag{27}$$

For further forward slip, we would require $S(x) = -fN(x) > 0$, which cannot be fulfilled. For backslip we require $S(x) = fN(x) < 0$, x ϵ new slip zone, which may be solved for λ, giving

$$\lambda_{crit} = \frac{2fg_2}{fg_2 - g_1}. \tag{29}$$

If λ is less than this critical value, the crack faces remain locked. Figure 7 shows the variation of λ_{crit} with f and depth. It is seen that λ_{crit} decreases monotonically with x, and thus backslip will always start at the deeper crack tip. Also, it is interesting to

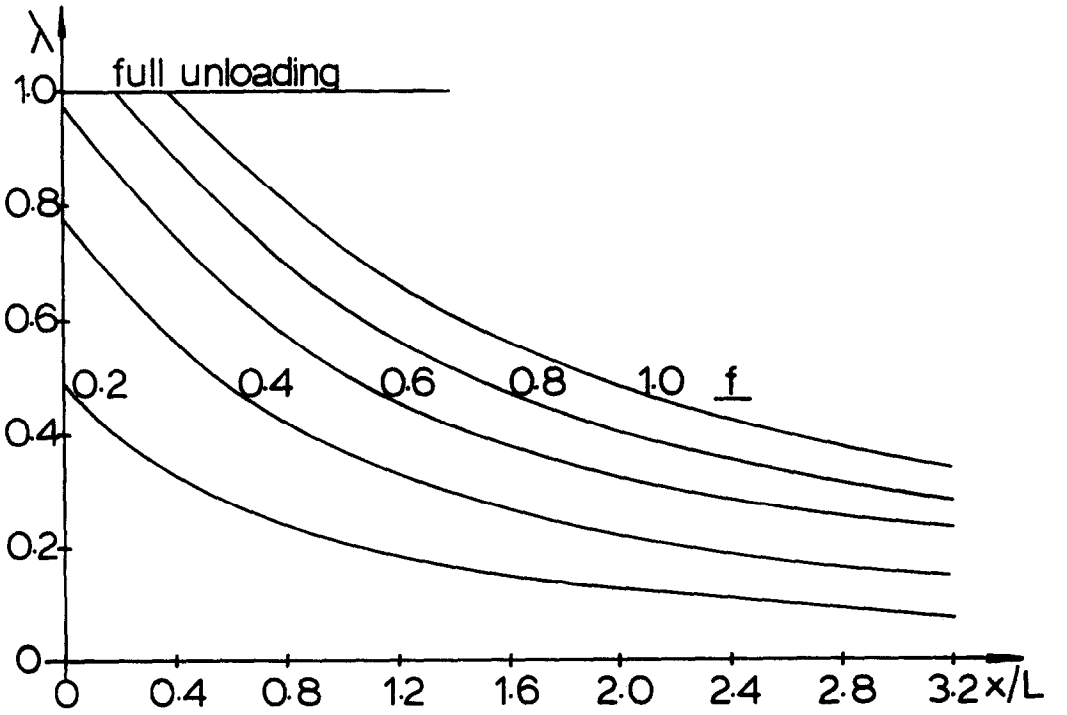

Fig. 7. Fraction of applied load that must be relaxed to initiate backslip.

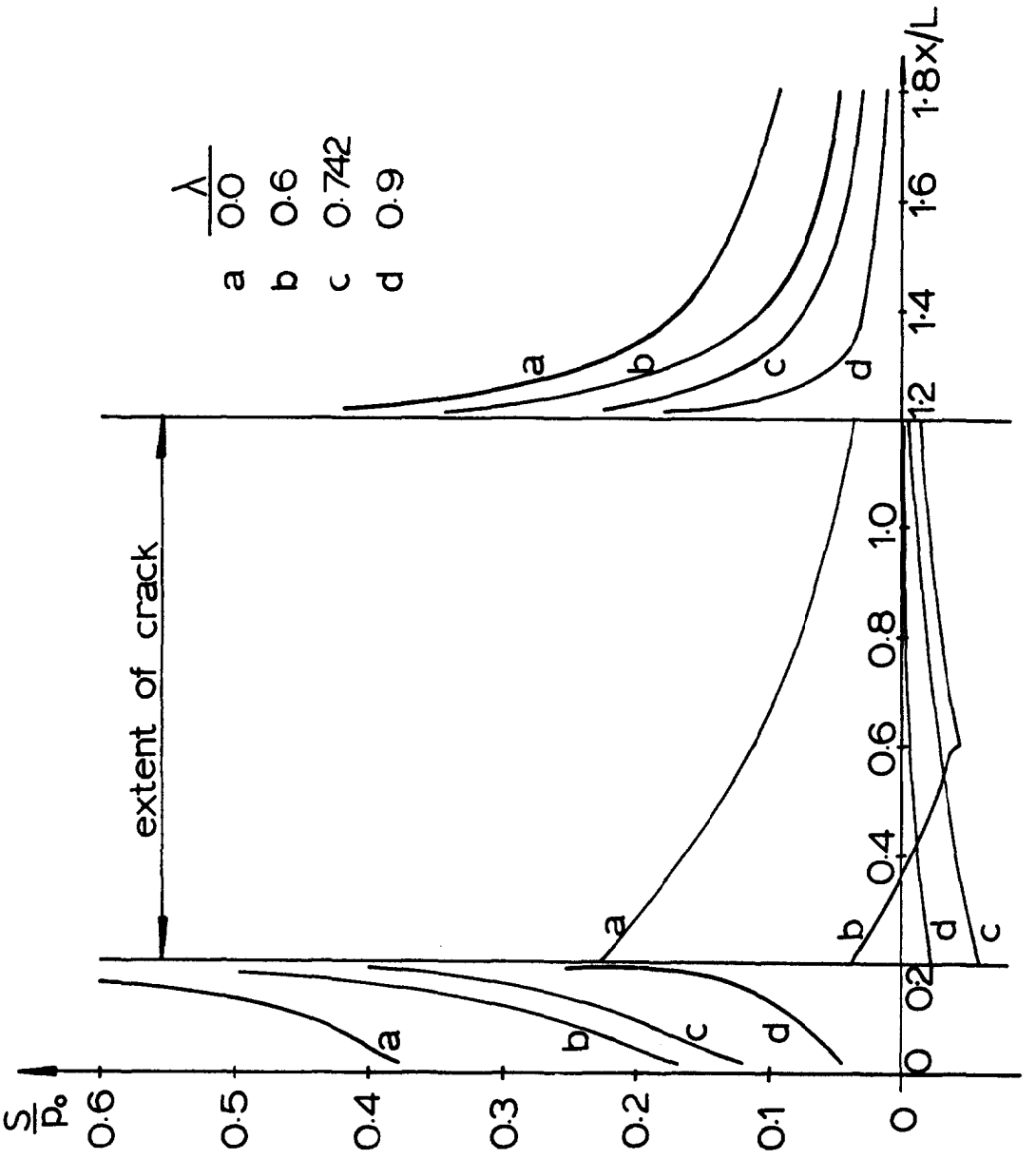

Fig. 8. Stress present before and during the unloading of a typical case I-type crack.

note that those cracks requiring the removal of all load to initiate backslip ($\lambda \rightarrow 1$) correspond to those having a vanishingly small slip zone, as predicted by Fig. 5.

For finite backslip, the integral equation to be solved is

$$fN(x) = S(x) = -fN^*(x) - \lambda p^* g_1(x) + \frac{2\mu}{\pi(\kappa + 1)} \int_c^b \hat{B}_x(\xi) K(x, \xi)\, d\xi \qquad (30)$$

or in normalized form

$$\frac{1}{\pi} \int_{-1}^{+1} w(r)\hat{\phi}(r)\, K(r, s)\, dr = \frac{1}{\delta} [g_1 + f(2 - \lambda)g_2]. \qquad (31)$$

This equation was treated by the same method described for case II. The specific example chosen was a crack extending from $a/L = 0.26$ to $b/L = 1.26$ with a value of $f = 0.6$. Figure 8 shows the resultant stress distribution after loading and during the unloading cycle. In this case, backslip started at $\lambda = 0.4581$, and gradually extended across the entire crack, which occurred at $\lambda = 0.7416$. For greater values of λ, the integral eqn (31) remains identical, but it should be remembered that it is now singular at both ends, and needs to be discretized by the techniques described for case I.

The value of the shear traction at $x = 0$ depends on the limiting sequence chosen in the bilateral solution. For ϵ small but finite, the traction drops rapidly to zero when x is close to zero.

CONCLUSION

An analysis of the possible loading regimes of a vertical embedded or surface-breaking crack has been demonstrated. For the most frequently occurring geometry, viz. a surface-breaking crack, comprehensive values of the stress intensity factor are presented. These are expected to be of value in predicting the durability of surfaces under repeated impact loading. It is shown that there are no residual internal stresses present after a load cycle, so that there is no possibility of shakedown. Also, the steady-state range of stress intensity factor is the same as that induced in the first cycle.

Acknowledgement—David Hills would like to acknowledge gratefully the support received from the English Speaking Union during this work.

REFERENCES

1. M. Comninou and J. R. Barber, Frictional slip between a layer and substrate due to a periodic tangential force. *Int. J. Solids Structures* **19**, 533–539 (1983).
2. M. Comninou, J. R. Barber and J. Dundurs, Interface slip caused by a surface load moving at a constant speed. *Int. J. Mech. Sci.* **25**, 41–46 (1983).
3. F.-K. Chang, M. Comninou and J. R. Barber, Slip between a layer and a substrate caused by a normal force moving steadily over the surface. *Int. J. Mech. Sci.* **50**, 803–809 (1983).
4. D. Schmueser, M. Comninou and J. Dundurs, Frictional slip between a layer and substrate. *J. Engng Div. ASCE* **107**, 1103–1118 (1981).
5. F.-K. Chang, M. Comninou, S. Sheppard and J. R. Barber, The subsurface crack under conditions of slip and stick caused by a surface normal force. *J. Appl. Mech.* **51**, 311–316 (1984).
6. S. L. Rice, Reciprocating impact wear testing apparatus. *Wear* **45**, 85–95 (1977).
7. P. R. Edwards, The application of fracture mechanics to predicting fretting fatigue. In *Fretting Fatigue* (Edited by R. B. Waterhouse), Chap. 3. Applied Sci. Pub. Ltd., London (1981).
8. J. Dundurs and G. P. Sendeckyj, Behavior of an edge dislocation near a bimetallic interface. *J. Appl. Phys.* **36**, 3353–3354 (1965).
9. J. Dundurs and T. Mura, Interaction between an edge dislocation and a circular inclusion. *J. Mech. Phys. Solids* **12**, 177–189 (1964).
10. F. Erdogan, G. D. Gupta and T. S. Cook, Numerical solution of singular integral equations. In *Methods of Analysis and Solutions of Crack Problems* (Edited by G. C. Sih), Chap. 7. Noordhoff, Leyden (1973).
11. J. Dundurs and M. Comninou, Some consequences of inequality conditions in contact and crack problems. *J. Elasticity* **107**, 71–82 (1979).
12. S. Krenk, On the use of the interpolation polynomial for solutions of singular integral equations. *Quart. J. Appl. Math.* **32**, 479–484 (1975).
13. G. D. Gupta and F. Erdogan, The problem of edge cracks in an infinite strip. *J. Appl. Mech.* **41**, 1001–1006 (1974).